Bioorganic & Medicinal Chemistry Letters 22 (2012) 733–737

Contents lists available at SciVerse ScienceDirect

Bioorganic & Medicinal Chemistry Letters

journal homepage: www.elsevier.com/locate/bmcl

Indole RSK inhibitors. Part 1: Discovery and initial SAR

Stephen J. Boyer [a,*], Jennifer Burke [a], Xin Guo [a], Thomas M. Kirrane [a], Roger J. Snow [a], Yunlong Zhang [a], Chris Sarko [a], Lida Soleymanzadeh [a], Alan Swinamer [a], John Westbrook [a], Frank DiCapua [a], Anil Padyana [a], Derek Cogan [a], Amy Gao [a], Zhaoming Xiong [a], Jeffrey B. Madwed [b,†], Mohammed Kashem [a], Stanley Kugler [a], Margaret M. O'Neill [b]

[a] Department of Medicinal Chemistry, Boehringer-Ingelheim Pharmaceuticals, Inc., 900 Ridgebury Road, PO Box 368, Ridgefield, CT 06877, United States
[b] Department of CardioMetabolic Diseases Research, Boehringer-Ingelheim Pharmaceuticals, Inc., 900 Ridgebury Road, PO Box 368, Ridgefield, CT 06877, United States

ARTICLE INFO

Article history:
Received 28 July 2011
Revised 5 October 2011
Accepted 7 October 2011
Available online 14 October 2011

Keywords:
RSK
MAPKAP-K1
Kinase inhibitor

ABSTRACT

A series of inhibitors for the 90 kDa ribosomal S6 kinase (RSK) based on an 1-oxo-2,3,4,5-tetrahydro-1*H*-[1,4]diazepino[1,2-*a*]indole-8-carboxamide scaffold were identified through high throughput screening. An RSK crystal structure and exploratory SAR were used to define the series pharmacophore. Compounds with good cell potency, such as compounds **43**, **44**, and **55** were identified, and form the basis for subsequent kinase selectivity optimization.

Myocardial ischemia rapidly sets in motion a series of pathological processes, most significantly intracellular acidosis that arises from anaerobic glycolytic metabolism. The sodium–hydrogen exchanger (NHE) plays a critical role in regulating cellular pH post-MI by removing protons while concomitantly internalizing Na^+.[1] However, what begins as a protective response later transforms into a maladaptive process; elevated cellular Na^+ decreases Ca^{2+} efflux, ultimately leading to Ca^{2+} overload and cardiac hypertrophy.[2] Inhibitors of NHE have been shown to reverse this sequence of events, and have demonstrated efficacy in preclinical models of ischemia-reperfusion injury and heart failure.[3]

Unfortunately, NHE inhibitors have also been associated with adverse clinical events.[4] Moreover, the NHE inhibitor zoniporide was found to be neurotoxic.[5] One possible explanation for the undesirable effects of NHE inhibitors is that the compounds not only block NHE during times of stress, but also completely inhibit the protein's housekeeping function. An alternative approach for a cardioprotective agent could be to reduce the activation of NHE, while retaining the basal activity necessary for cellular pH maintenance.

The 90 kDa ribosomal S6 kinase (RSK, also known as mitogen-activated protein kinase-activated protein kinase-1 [MAPKAP-K1]) has been shown to be one such NHE activating factor and a potential point for therapeutic intervention.[6] A member of the ACG kinase subfamily, the RSK family consists of four human isoforms, RSK 1–4.[7] The RSK 1–3 isoforms have a high degree of homology, are ubiquitously expressed, and have all been shown to stimulate NHE1 via phosphorylation in vitro[8]; RSK4 appears to demonstrate different pharmacology.[9] A feature atypical for most kinases, RSK possesses two functionally distinct kinase domains: an N-terminal domain homologous to other ACG kinases, and a C-terminal autophosphorylation domain homologous to the calcium/calmodulin-dependent protein kinases.[10]

Few small molecule RSK inhibitors have been documented in the literature, most notably fmk, SL0101, and BI-D1870.[11] Additionally, RSK has appeared in the selectivity profiles for other kinase inhibitors.[12] As part of an ongoing program directed at the NHE pathway,[13] we undertook a high-throughput screen (HTS) to identify novel scaffolds for inhibitors of the RSK N-terminal kinase domain. Indole **1** (Fig. 1) is representative of an attractive cluster from the hitset. Interestingly, selected members were found previously to be MAPKAP-K2 (MK2) inhibitors.[14]

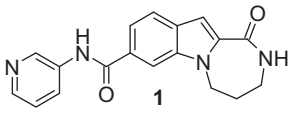

Figure 1. An HTS hit from the indole series.

* Corresponding author at present address: Global Regulatory Sciences, Bristol-Myers Squibb, 5 Research Parkway, Wallingford, CT 06492, United States.
E-mail address: stephen.boyer.b@gmail.com (S.J. Boyer).
† Present address: Department of Cardiovascular Diseases, Merck & Co. Inc., 126 E. Lincoln Avenue, PO Box 2000, Rahway, NJ 07065, United States.

0960-894X/$ - see front matter © 2011 Elsevier Ltd. All rights reserved.
doi:10.1016/j.bmcl.2011.10.030

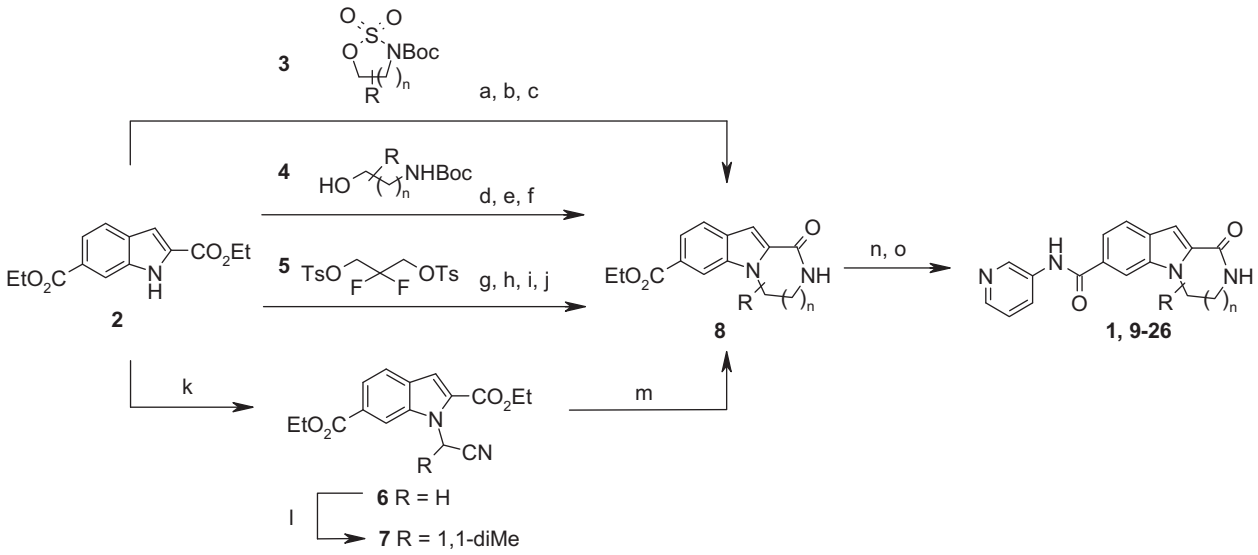

Scheme 1. Reagents and conditions: (a) NaH, DMF, 0 °C—rt, 48–72 h; (b) TFA, CH_2Cl_2, 1 h, rt; (c) K_2CO_3, EtOH, reflux, 1–4 h, 20–66% (three steps); (d) DIAD, Ph_3P, THF, 16–60 h, rt; (e) TFA, CH_2Cl_2, 1–2 h, rt; (f) K_2CO_3, Et_3N, EtOH, reflux, 1–4 h, 15–66% (three steps); (g) K_2CO_3, DMF, 135 °C, microwave, 1 h, 38%; (h) NaN_3, DMF, 95 °C, 40 h; (i) H_2, 10% Pd/C, MeOH/CH_2Cl_2 (1:1 v/v), 3.5 h; (j) K_2CO_3, Et_3N, EtOH, 80 °C, 16 h, 15–66% (three steps); (k) $BrCH_2CN$, K_2CO_3, DMF, 60–80 °C, 4–6 h, 84–96%; (l) NaHMDS, MeI, THF, 0 °C—rt, 24 h, 61%; (m) H_2, PtO_2/EtOH or Raney Ni/water, 85–95%; (n) 1 M NaOH, EtOH, 80 °C, 2 h, 58–96%; (o) 3-aminopyridine, PyBOP, Et_3N, DMF, 30–40% or 3-aminopyridine, TBTU, Et_3N, DMF, 40–75%.

Although we postulated the binding modes would be similar,[15] early SAR for RSK and MK2 appeared divergent, and thus, the indole series offered an attractive starting point.

The synthesis of indole series analogs proceeded through the indole lactam intermediate **8** (Scheme 1). Beginning with indole diester **2**,[14a] the lactam was assembled through one of four alternative routes that allowed access to a broad range of ring substituents. The cyclic sulfamidate[16] **3** (n = 1 or 2) was used to synthesize the corresponding intermediate **8** en route to compounds **9**, **12**, **13**, **21**, and **23**–**25** (Table 1) through a ring opening, deprotection and cyclization sequence. Alternatively, Mitsunobu reaction of the Boc-protected amino alcohol **4** (n = 1) with indole **2**, deprotection, and subsequent cyclization furnished intermediate **8** toward compounds **10**, **14**, and **16**–**19**. Mono displacement of ditosylate **5**,[17] installation of the lactam nitrogen, and cyclization provided the difluorinated intermediate **8** leading to compound **15**. In another approach, indole **2** was alkylated with bromoacetonitrile. The resultant nitrile **6** could either be directly carried on toward compound **20** via a one step hydrogenation/cyclization, or alkylated to afford the geminal di-methyl intermediate **7** necessary for compound **22**. Once in hand, the substituted indole lactam **8** was readily converted to final products following hydrolysis and coupling with the 3-aminopyridine left-hand side (LHS). The syntheses of compounds **1**, **11**, and **26** have been described previously.[14b]

Table 1
Piperazinone and diazepinone SAR

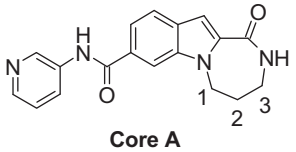

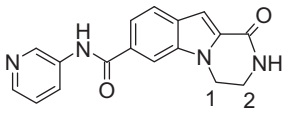

Compound	Core	Substituent	RSK2 IC_{50}[a] (nM)	HLR-CREB IC_{50}[19] (nM)
1	A	—	240	1940
9	A	1-Me	41	890
10	A	2-Me	1200	4890
11	A	2-CH_2NH_2	1800	
12	A	1,2-*cis* Di Me	240	
13	A	1,2-*trans* Di Me	1100	
14	A	2,2-Di Me	4600	
15	A	2,2-Di F	1700	
16	A	2-*spiro c*-Pr	410	
17	A	2-*spiro c*-Bu	3300	
18	A	2-*spiro* (4-THP)	>10000	
19	A	3-Me	2500	
20	B	—	730	>10000
21	B	1-Me	170	1630
22	B	1,1-Di Me	210	1550
23	B	1,2-*cis* Di Me	45	840
24	B	1,2-*trans* Di Me	871	
25	B	2-Me	350	
26	B	2-CH_2NH_2	970	

[a] Values are means of at least two experiments, standard deviation is typically 50% of the reported value.

With the high degree of homology between the RSK family members and the general lack of RSK isoform selectivity observed during early optimization of several other lead series, we chose to develop SAR primarily against RSK2.[18] Additionally, we used a proprietary X-ray crystal structure of RSK2 for novel analog design. Affinity for other RSK isoforms was periodically confirmed in a broad selectivity panel for key compounds, and binding interactions were corroborated with homology models of RSK1 and RSK3.

The structure of compound **1** docked into RSK2 is shown in Figure 2a. Members of the indole series are thought to form key hydrogen bonds with RSK2; the three within 2.2 Å are shown as yellow lines. These were corroborated by SAR developed during hit evaluation. The amide carbonyl anchors the molecule to the backbone N-H of Leu150 in the hinge region. An additional strong hydrogen-bonding interaction appears between the lactam carbonyl and the catalytic Lys100 side chain nitrogen. A third, out of plane hydrogen bond connects the lactam nitrogen with the side chain carboxylate of Asp211. Analogs lacking any of these three critical elements of the indole series pharmacophore were found to be poor inhibitors of RSK2. Additionally, the LHS amide substituent binds in a lipophilic pocket bounded in part by Phe149, and engages in π-stacking with Phe357.

Bound to RSK2 in this manner, the seven-membered indole lactam fits tightly into the ATP pocket with limited room for substitution (Fig. 2b). The majority of ring substituents led to a loss

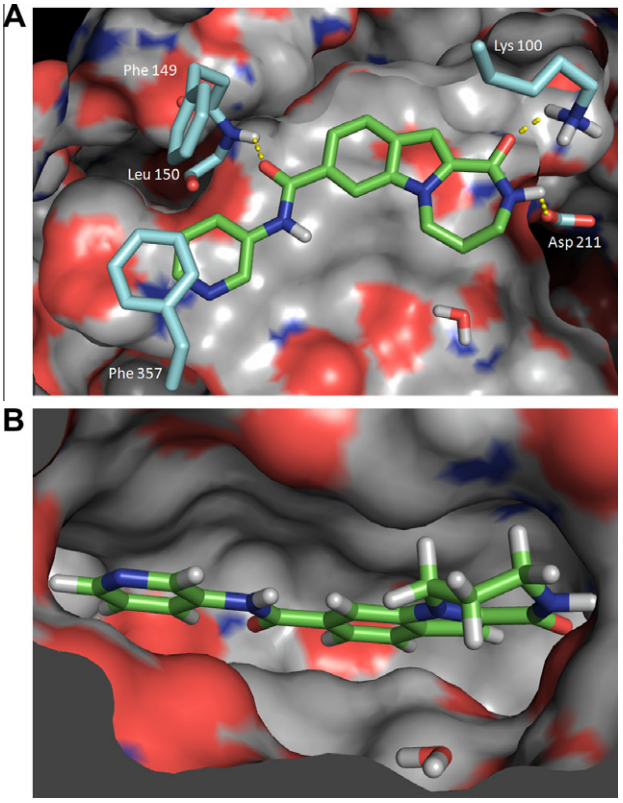

Figure 2. Docking of **1** into a crystal structure of RSK2 [30-350] (2.9 Å resolution, Boehringer-Ingelheim unpublished results). The binding mode is based on an X-ray structure for an analogous compound bound to MK2.[15]

in potency (Table 1); however, introduction of a methyl alpha- to the indole provided a six-fold improvement in RSK2 IC_{50} (**9**). This can be understood by the allylic 1,3-strain between the α-methyl and the indole 7-position C–H, which forces the α-methyl to adopt an axial conformation and places it into a lipophilic indentation in the roof of the pocket. Substitution at the adjacent β-position substantially decreased potency (**10**). In this region, the roof of the pocket appears to be less accommodating toward an equatorial substituent. Alternatively, axial orientation of the β-substituent either displaces the nearby bound water or clashes with the roof in the ring conformation not shown in Figure 2b. Attempts to directly address the bound water through hydrogen-bonding substituents were unsuccessful, as demonstrated by compound **11**.

Interestingly, α,β-vicinal disubstitution could compensate for the potency loss due to β-monosubstitution, with the *cis*-diastereomer **12** favored over the corresponding *trans*- (**13**). This diastereomeric preference reinforces the binding hypothesis: compound **12** allows for the preferred axial methyl orientation without bound water displacement, while compound **13** can only adopt conformations with disfavored interactions. Geminal disubstitution of the central methylene also reduced potency (**14–18**). Reduced steric demand at this position has a less detrimental effect (compare **14** with **16**).

Substituents next to the lactam nitrogen were also not tolerated (compound **19**), consistent with the proposed binding mode which places this methylene in close proximity to the wall of the binding pocket.

The SAR trends in six-membered lactam analogs were in part consistent with those observed for the seven-membered counterparts: methyl substituents alpha- to the indole improved potency (compounds **20**–**22**), and *cis*-α,β disubstitution was preferred over *trans*- (compare **23** and **24**). However, in contrast to the seven-membered lactams, a β-methyl substituent in **25** led to moderate potency increase. This is likely due to a different orientation of the smaller ring within the pocket, which avoids the negative clash with the wall, and also allows the methyl to interact constructively with the lipophilic roof indentation. Similar to the 7-membered lactam, the β-aminomethyl derivative **26** did not provide an expected potency boost through a bridge to the bound water.

Having explored the lactam ring SAR, we then turned toward amide LHS optimization (Table 2). Throughout, we held the more potent seven-membered lactam constant while seeking to define interactions within the lipophilic pocket necessary for RSK inhibition. It was quickly established that a π-stacking interaction with Phe357 is another critical element of the indole series pharmacophore, as demonstrated by the poor activity of unsubstituted amide **27** and cyclohexyl analog **28**. Moreover, the pyridyl nitrogen (**1**) does not appear to be critical for binding, as the corresponding phenyl derivative **29** is equipotent.

Probing space around the aromatic LHS with a chlorine, the *para*- (**30**) and *meta*- (**31**) derivatives were found to be tolerated, while the *ortho*- analog **32** significantly lost potency. This effect ap-

Table 2
SAR of amide substituent—six membered rings

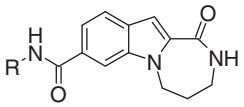

Compound	R	RSK2 IC_{50} (nM)	HLR-CREB IC_{50} (nM)
27	H	9100	
28		>10000	
29		290	1930
30	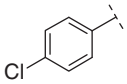	180	
31	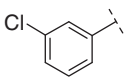	270	
32	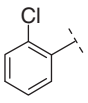	6000	
33	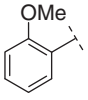	400	
34	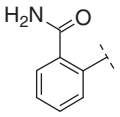	21	560
35		34	620
36		220	2630
37		>10000	
38	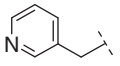	>10000	>10000
39	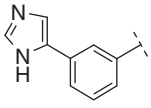	52	

pears to be driven by a steric clash between the *ortho*- substituent and the amide that forces the LHS to twist out of plane with the indole. As seen in Figure 2b, the lipophilic pocket is narrow and would be unable to accommodate more demanding functionality. In contrast, an *ortho*-methoxy substituent capable of enforcing planarity via an intramolecular hydrogen bond to the amide had limited impact on potency (**33**). A boost in potency was observed for the *ortho*-amide **34**, which may also provide an interaction beyond the intramolecular hydrogen bond by reaching out to Asp154 on the lip of the ATP pocket.

Similar conformational effects on IC_{50} were observed for other heterocycles, in this case driven by electrostatic repulsion between Leu150 of RSK and the LHS rather than sterics. Although the 4-pyridyl regioisomer **35** gains potency relative to the HTS hit **1** and the 2-pyridine regioisomer **36** is equipotent, the 2-pyrimidine analog **37** surprisingly loses affinity for RSK. We reasoned that a repulsive interaction between the two pyrimidine nitrogens and the Leu150 backbone carbonyl would either lead **37** to adopt a twisted conformation upon binding analogous to the unbound conformation of **32**, or significantly disfavor binding. In this context, pyridines **1** and **36** are free to adopt an orientation that points the ring nitrogen away from the backbone, while **35** has no repulsive interaction with RSK.

We also targeted the space in the lipophilic pocket off of the phenyl *meta*-position. Chain extension to better position the pyridyl deeper into the pocket led to a complete loss in potency (**38**). It appears that maintaining aromatic LHS π-stacking while expanding into the lipophilic pocket is critical. Thus, we carried out a library directed at validating the hypothesis. The imidazole derivative **39** is a representative example that provided a five-fold boost in IC_{50} relative to the parent phenyl; however, it came at the expense of a modest reduction in ligand efficiency.

Five membered heterocycle LHS offered a potential path to more ligand efficient compounds (Table 3). But, thiazole **40**, a bioisostere of pyridine **36**, lost 10-fold RSK potency. We hypothesized that electrostatic repulsion impacts thiazole **40** binding, similar to that of **37**, and then chose to introduce a heterocycle that could constructively interact with the Leu150 backbone carbonyl. Gratifyingly, **41** offered a 10-fold boost in potency, and an additional hydrogen bonding opportunity from the imidazole N–H. The methylated analog **42** prevents the hydrogen bond formation with corresponding loss of potency. Complicating the interpretation, it also introduces a substituent adjacent to the amide that leads to a conformational change and analogous to *ortho*-chlorophenyl **32**. Interestingly, a bidentate interaction is not necessary to increase affinity for RSK, as demonstrated by isoxazole **43** and pyrazole **44**.

In general, the rank order for potency was the same for both the primary soluble kinase and for cellular mechanistic phosphorylation assays, although physicochemical properties were found to impact cell potency in some cases. While pyrazoles **44** and **45** are equipotent in the kinase assay, the methyl of pyrazole **44** appears to allow better cell penetration. Specifically, permeability as measured in the PAMPA assay was found to be 10-fold lower for **45** than **44**.

The interplay of electronic and steric factors on potency is well illustrated by the 3-aminopyrazole regioisomers **46**–**48**. Electrostatic repulsion orients the pyrazole LHS of **46** such that the trajectory for the methyl substituent differs from that of **43** and **44**. Ultimately, this leads to a clash with the lipophilic pocket near the entrance and loss in potency. Removal of the methyl (**47**) resolves the conflict, while the other regioisomer (**48**) further confirms that adjacent LHS substitution is disfavored.

Fused ring systems provided further insight into the LHS SAR (Table 4). We observed a potency boost through increased lipophilicity with quinoline **49**, and found that the lipophilic pocket could accommodate relatively large LHS such as the pyrazolopyridine **50**. Compounds **51** and **52**, direct analogs of the monocycles **36** and **40**,

Table 3
SAR of amide substituent—five membered rings

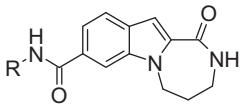

Compound	R	RSK2 IC_{50} (nM)	HLR-CREB IC_{50} (nM)
40		2200	
41		26	290
42		2200	
43	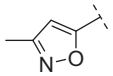	19	200
44	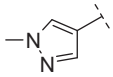	11	790
45	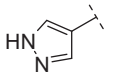	43	>10000
46		540	
47		93	
48		>1000	

Table 4
SAR of amide substituent—fused ring systems

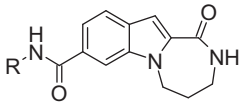

Compound	R	RSK2 IC_{50} (nM)	HLR-CREB IC_{50} (nM)
49	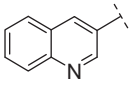	34	340
50	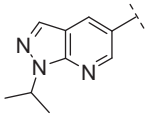	53	840
51	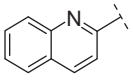	68	1130
52	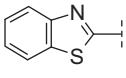	>10000	
53	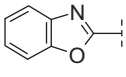	367	>10000
54	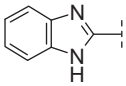	4	>10000
55	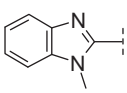	9	200

confirm the previous observation that electrostatic repulsion has a deleterious effect on potency. It is noteworthy that although ring fusion significantly improved the potency of quinoline **51** it was not sufficient to overcome the negative conformational effects for benzothiazole **52**.

With the LHS SAR apparently well established, we were surprised to find that the benzoxazole **53** demonstrated modest RSK inhibition. This counterintuitive result can be explained through the imino–amino tautomeric equilibrium of the LHS. In the case of **53**, the aminobenzoxazole spends a portion of its time in the imino tautomer, effectively replacing a ligand-receptor repulsive interaction with a hydrogen bonding opportunity. The hypothesis is further supported by the aminobenzimidazoles **54** and **55**, which behave differently than their unfused counterparts. While **54** showed the expected increase in potency compared to **41** that can be attributed to ring fusion, the methyl analog **55** maintained excellent potency, in stark contrast to **42**. In this case, it appears that the aminobenzimidazole LHS of **55** tautomerizes to offer the same hydrogen bonding interaction as the unalkylated analog. N-methylation also provides **55** with better cell penetration measured by cell assay potency.

We were also interested in the kinome selectivity of the indole series, particularly given the chronic disease indication and the potential for off-target kinase inhibition that could lead to safety concerns. During the early optimization phase described in this report, we found most compounds to be highly selective against a limited panel of kinases including Aurora A, CHEK1, GSK3β, MEK5, and STK33. Having defined critical elements of the indole series SAR and also identified compounds with good cell potency, such as isoxazole **43**, pyrazole **44**, and benzimidazole **55**, we turned toward optimization of selectivity against a broader panel of kinases. These results will be reported in a subsequent communication.[20]

Acknowledgments

The authors would like to thank I. Mugge for discussions, J. Wolak and S. Marques for help providing HTS data, and D. Brennan for RSK crystals

References and notes

1. Karmazyn, M.; Sawyer, M.; Fliegel, L. *Curr. Drug Targets Cardiovasc. Haematol. Disord.* **2005**, *5*, 323.
2. Nakamura, T. Y.; Iwata, Y.; Arai, Y.; Komamura, K. Wakabayashi *Circ. Res.* **2008**, *103*, 891.
3. (a) Karmazyn, M.; Kilic, A.; Javadov, S. *J. Mol. Cell Cardiol.* **2008**, *44*, 647–653; (b) Karmazyn, M.; Gan, X. T.; Humphreys, R. A.; Yoshida, H.; Kusumoto, K. *Circ. Res.* **1999**, *85*, 777.
4. For example, development of cariporide was halted due to higher incidence of stroke: Mentzer, R. M.; Bartels, C.; Bolli, R.; Boyce, S.; Buckberg, G. D.; Chaitman, B.; Haverich, A.; Knight, J.; Menasche, P.; Myers, M. L.; Nicolau, J.; Simoons, M.; Thulin, L.; Weisel, R. D. *Ann. Thorac. Surg.* **2008**, *85*, 1261.
5. (a) Petterson, J. C.; Chouinard, L.; Kerlin, R. L.; Groom, S. N.; Botts, S.; Arezzo, J. C.; Boucher, M. A.; Frazier, D. E.; Buchholz, A. R. *Toxicol. Pathol.* **2008**, *36*, 608; (b) Liu, C.-N.; Somps, C. J. *Toxicol. Sci.* **2008**, *103*, 346.
6. (a) Moor, A. N.; Gan, X. T.; Karmazyn, M.; Fliegel, L. *J. Biol. Chem.* **2001**, *276*, 16113; (b) Maekawa, N.; Abe, J.-I.; Shishido, T.; Itoh, S.; Ding, B.; Sharma, V. K.; Sheu, S.-S.; Vlaxall, B. C.; Berk, B. C. *Circulation* **2006**, *113*, 2516; (c) Avkiran, M.; Cook, A. R.; Cuello, F. *Curr. Opin. Pharmacol.* **2008**, *8*, 133.
7. (a) Anjum, R.; Blenis, J. *Nat. Rev. Mol. Cell Biol.* **2008**, *9*, 747–758; (b) Carriere, A.; Ray, H.; Blenis, J.; Roux, P. P. *Front. Biosci.* **2008**, *13*, 4258.
8. Roberts, N. A.; Haworth, R. S.; Avkiran, M. *Br. J. Pharmacol.* **2005**, *145*, 477.
9. Dümmler, B. A.; Hauge, C.; Silber, J.; Yntema, H. G.; Kruse, L. S.; Kofoed, B.; Hemmings, B. A.; Alessi, D. R.; Frödin, M. *J. Biol. Chem.* **2005**, *280*, 13304.
10. (a) Malakhova, M.; Tereshko, V.; Lee, S.-Y.; Yao, K.; Cho, Y.-Y.; Bode, A.; Dong, Z. *Nat. Struct. Mol. Biol.* **2008**, *15*, 112; (b) Ikuta, M.; Kornienko, M.; Byrne, N.; Reid, J. C.; Mizuarai, S.; Kotani, H.; Munshi, S. *Protein Sci.* **2007**, *16*, 2626.
11. Nguyen, T. L. *Anti-Cancer Agents Med. Chem.* **2008**, *8*, 710.
12. (a) Stavenger, R. A.; Cui, H.; Dowdell, S. E.; Franz, R. G.; Gaitanopoulos, D. E.; Goodman, K. B.; Hilfiker, M. A.; Ivy, R. L.; Leber, J. D.; Marino, J. P.; Oh, H.-J.; Viet, A. Q.; Xu, W.; Ye, G.; Zhang, D.; Zhao, Y.; Jolivetter, L. J.; Head, M. S.; Semus, S. F.; Elkins, P. A.; Kirkpatrick, R. B.; Dul, E.; Khandekar, S. S.; Yi, T.; Jung, D. K.; Wright, L. L.; Smith, G. K.; Behm, D. J.; Doe, C. P.; Bently, R.; Chen, Z. X.; Hu, E.; Lee, D. *J. Med. Chem.* **2007**, *50*, 2; (b) Lovering, F.; Kirincich, S.; Wang, W.; Combs, K.; Resnick, L.; Sabalski, J. E.; Butera, J.; Liu, J.; Parris, K.; Telliez, J. B. *Bioorg. Med. Chem.* **2009**, *17*, 3342.
13. Huber, J. D.; Guo, X.; Soleymanzadeh, F.; Swinamer, A.; Kennedy, C.; Kaplita, P.; Nagaraja, N.; Eickmeier, C.; Madwed, J. B.; DeLombaert, S.; Eldrup, A. B. Abstracts of Papers, 241st National Meeting of the American Chemical Society, Anaheim, CA, **2011**, Abstract MEDI-23.
14. (a) Goldberg, D. R.; Choi, Y.; Cogan, D.; Corson, M.; DeLeon, R.; Gao, A.; Gruenbaum, L.; Hao, M.-H.; Joseph, D.; Kashem, M. A.; Miller, C.; Moss, N.; Netherton, M. R.; Pargellis, C. P.; Pelletier, J.; Sellati, R.; Skow, D.; Torcellini, C.; Tseng, Y.-C.; Wang, J.; Wasti, R.; Werneburg, B.; Wu, J. P.; Xiong, Z. *Bioorg. Med. Chem. Lett.* **2008**, *18*, 938; (b) Xiong, Z.; Gao, A.; Cogan, D. A.; Goldberg, D. R.; Hao, M.-H.; Moss, N.; Pack, E.; Pargellis, C.; Skow, D.; Trieselmann, T.; Werneburg, B.; White, A. *Bioorg. Med. Chem. Lett.* **2008**, *18*, 1994.
15. A crystal structure for a related series bound to MK2a has been published: Wu, J.-P.; Wang, J.; Abeywardane, A.; Andersen, D.; Emmanuel, M.; Gautschi, E.; Goldberg, D. R.; Kashem, M. A.; Lukas, S.; Mao, W.; Martin, L.; Morwick, T.; Moss, N.; Pargellis, C.; Patel, U. R.; Patnaude, L.; Peet, G. W.; Skow, D.; Snow, R. J.; Ward, Y.; Werneburg, B.; White, A. *Bioorg. Med. Chem. Lett.* **2007**, *17*, 4664.
16. Alker, D.; Doyle, K. J.; Harwood, L. M.; McGregor, A. *Tetrahedron: Asymmetry* **1990**, *1*, 877.
17. Binsch, G.; Eliel, E. L.; Mager, S. *J. Org. Chem.* **1973**, *38*, 4079.
18. Inhibition of soluble RSK2 phosphorylation activity was determined with a luminescent assay format similar to that described in: Zegzouti, H.; Zdanovskaia, M.; Hsiao, K.; Goueli, S. A. *Assay Drug Dev. Technol.* **2009**, *7*, 560.
19. Inhibition of the phosphorylation of the transcription factor CREB (cAMP Response Element Binding) by RSK2 in cells was determined according to the method described in: Boyer, S.; Gao, A.; Guo, X.; Kirrane, T.; Sarko, C.; Snow, R.; Soleymanzadeh, F.; Zhang, Y. WO2011071716.
20. Kirrane, T. K.; Boyer, S. J.; Burke, J.; Guo, X.; Snow, R. J.; Soleymanzadeh, L.; Swinamer, A.; Zhang, Y.; Madwed, J. B.; Kashem, M.; Kugler, S.; O'Neill, M. M. *Biorg. Med. Chem. Lett.* **2011**. doi:10.1016/j.bmcl.2011.10.029.